Inf. Téc. (2016) 80 (2) p 128-140 ISSN 0122-056X | e-ISSN 2256-5035

Mineralogy of the leaching process in refractory minerals with thiosulphate solutions[1]

Mineralogía del proceso de lixiviación de oro en minerales refractarios con soluciones de tiosulfato[1]

Juan David Ospina Correa[2]
Juan Guillermo Osorio Cachaya[3]
Carlos Mario Serna Zuluaga[4]
Erica Mejía Restrepo[5]
Carlos Enrique Giraldo Vélez[6]
José Alejandro Posada Montoya[7]

Received: 26- 08 - 2016 Acepted: 20-11-2016

[1] Research concluded: Mineralogy of the Gold Leaching Process of Refractory Minerals in Thiosulphate solutions, April 1, 2016 - September 30, 2016. Pascual Bravo University Institution.

[2] Colombiano Ing., De Materiales, M.Eng Materials and Processes, Dr (C) Ingeniería, Ciencia y Tecnología de Materiales. Group of Investigation and Environmental Innovation GIIAM. Pascual Bravo University Institution, Medellín., Colombia juan.ospina@pascualbravo.edu.co.

[3] Colombian. Ing. Geologist. Group of Investigation and Environmental Innovation GIIAM. Pascual Bravo University Institution, Medellín., Colombia juancachaya @ pascualbravo.edu.co.

[4] Colombian Eng., Materials, M.Eng (C) Materials and Processes. GIIAM Environmental Research and Innovation Group. University Institution Pascual Bravo, Medellín., Colombia. c.serna@pascualbravo.edu.co.

[5] Colombian Ing. Materiales, M.Eng Materials and Processes, Dr (C) Biotechnology. Man, project and city research group. Industrial Design Program, San Buenaventura University, Medellín, Colombia. erica.mejia@usbmed.edu.co.

[6] Colombian Industrial Engineer Group of Investigation and Environmental Innovation GIIAM. Pascual Bravo University Institution, Medellín., Colombia ce.giraldo @ pascualbravo.edu.co, ellín, Colombia. erica.mejia@usbmed.edu.co

[7] Colombian. Postdoctoral degree in Mechanical and Aerospace Engineering, Ph.D. in Aerospace Engineering, Aeronautical Specialist, Mechanical Engineer, Visiting Professor, Teaching Institution, Pascual Bravo University, Assistant Professor, Universidad Pontificia Bolivariana. Group of Investigation and Environmental Innovation GIIAM. University Institution Pascual Bravo, Medellín., Colombia. alejandro.posada @ pascualbravo.edu.co.

Summary

Mineralogy of processes is a tool that offers information of great utility for the modification of processes of obtaining gold to improve its efficiency. The objective of this work was to evaluate the mineralogy and the oxidation of the mineral in the process of leaching gold from refractory gold ore samples with thiosulfate solutions by analytical techniques such as Polarized Flat Light Optical Microscopy (MOLPP), Digital Treatment of TDI Images, Scanning Electron Microscopy (SEM / EDS) and X-ray Diffraction (XRD). The mineralogical characterization prior to the leaching process revealed the association, size and form of occurrence of each of the mineral phases, finding that the mineral used was composed mainly of pyrite in unigranular and sub -hedral crystals (58% of the sample); galena crystals (15% of the sample); crystals of sphalerite, chalcopyrite and arsenopyrite (7% of the sample); less than 1% free gold and aluminosilicate phases (19% of the sample). Fire tests showed 59 g / ton of gold and 70 g / ton of silver. After the leaching process accumulation of individual grains of pyrite with grooves of corrosion, decrease in their particle size was found, as well as the dissolution of the accompanying phases: sphalerite, chalcopyrite, galena and arsenopyrite. The presence of precipitated copper was not observed. It was necessary to perform an oxidant pretreatment of the ore, followed by a leaching, a gold release of up to 82% was achieved. The mineralogical characterization allowed to define adequate conditions for the recovery of gold.

Keywords: Mineralogical characterization; leaching; gold mining; refractory mineral; digital treatment of images.

Introduction

Mineralogy Process is a tool that offers very useful information for the modification of gold procurement processes; This has been approached very lightly in the literature, which may be due to the difficulty presented by the refractoriness of some minerals that hinder the recovery of gold. The Refractoriness in auropyritic minerals can be due to: (i) the presence of carbonaceous matter, (ii) formation of passivating films, (iii) gold particles finely disseminated in solid solution within the mineral matrix or gold in the crystalline structure of the sulfides, and (iv) various accompanying mineral phases, among others (Abrantes & Costa, 1996, Marsden & House, 2009).

The techniques commonly used for the benefit of refractory minerals such as amalgamation with mercury and subsequent treatment with cyanide have a low yield in gold recovery and rarely consider ore mineralogy for in situ modification of the solutions (Adams, 2005). Therefore, a great variety of unconventional methods have been developed to overcome the barriers that refractoriness imposes on the benefit processes (Amankwah & Pickles, 2009, Gudyanga, Mahlangu, Roman, Mungoshi, & Mbeve, 1999). For example, the recovery of gold from arsenic-pyritic minerals requires oxidative pretreatments in order to destroy the mineral matrix that contains gold encapsulation or decrease oxygen competition that increases costs in cyanidation (Climo, Watling, & Van Bronswijk , 2000; Hashemzadehfini, Ficeriová, Abkhoshk, & Shahraki, 2011). For this, the commonly proposed alternatives are preair conditioning, roasting, oxidation at high pressure and bacterial oxidation with Acidithiobacillus ferrooxidans and thiooxidans (Rohwerder & Sand, 2003). However, oxidant pretreatment processes have many disadvantages, such as: generation of SO and As O during roasting, high investment costs for the implementation of the oxidation under pressure, increase of periods of residence in reactors with agitation for biological oxidation, inhibition of microbial growth by the presence of arsenic in the solution, among others (Iglesias & Carranza, 1996, Leng et al., 2009). Some processes in alkaline solutions have been implemented for the oxidative dissolution of antimony and arsenic mineral concentrates. For example, Awe and Sandstrom (2010) used a mineral concentrate of tetraedrite-tenantite for the selective dissolution of arsenic and antimony and observed that the extraction of gold depends strongly on the amount of mineral, the concentration of ammonium hydroxide in the solution, the temperature and reaction time; the gold in these minerals is frequently encapsulated; this has been found for concentrates rich in arsenopyrite but the degree of surface corrosion of the mineral or the possible phase transformations during the process was not evaluated (Chen, Cabri, & Dutrizac, 2002).

On the other hand, Baláž and Achimovičová (2006) studied step leaching in alkaline systems of arsenic and antimony concentrates, prior mechanical activation of the mineral, finding that mechanical activation strongly influenced extraction, obtaining arsenic and antimony, 63% and 43% from the tetrahedrite. -tenantite and jamesonite respectively, and arsenic, 87% from the enargite. It should be noted that in these tests the particle size reached during the mechanical activation process is not evaluated. The research developed by Celep, Alp, & Deveci (2011); and Celep, Alp, Paktune, & Thibault (2011) showed the increase in the recovery of gold and silver by cyanidation with oxidant pretreatment, reaching recovery of 94% silver, 87% gold and 86% antimony removed with KOH, but they did not evaluate the degree of refractoriness of the mineral, that is, accompanying mineral phases such as arsenopyrite and stibin. Other studies, (Tongamp, Takasaki, & Shibayama, 2009) developed 95% arsenic removal from copper ores using alkaline leaching with NaHS at 95 ° C. During the process the arsenic outflow was not evaluated from the chalcopyrite, which is a mineral with a higher refractoriness than the chalcocite.

On the other hand, it has been found that pyrite and arsenopyrite are largely responsible for the refractoriness and increased cyanide consumption in gold beneficiation processes, which is why the morphological and textural transformations that occur during the oxidative dissolution of these Minerals are of great importance and a crucial part in the fundamental mechanism in the release of gold (Corkhill & Vaughan, 2009). However, little is known about the mineralogy of the process, which is a fundamental tool that allows the understanding of reaction mechanisms and thus an optimization of it (Márquez, 1999, Márquez, 1995).

The mineralogical characterization has been used as a tool to optimize the different benefit processes (Córdoba, Muñoz, Blázquez, González, & Ballester, 2008, Klauber, 2008). In this way, the knowledge and understanding of ore mineralogy and its influence on the final transformation of minerals are crucial for the design and operation of an industrial profit system (Marsden & House, 2009). Characteristics such as chemical composition of the phases, relative proportions, granulometric distribution, texture, type of intergrowth, degree of release and crystalline habits of the different minerals and their products in various stages of the process are factors basic for understanding the different points of the system (Muir & Aylmore, 2005).

With the use of thiosulfate solutions as a gold lixiviant in minerals with a high content of sulfides, gold solutions greater than 80% have been obtained (Zhang Senanayake, & Nicol, 2004; Zhang, 2008). In such minerals, metals such as gold are encapsulated in mineral phases, which require the application of previous oxidation processes (Mesa & Lapidus, 2015) to release the metal and maintain high levels of dissolution. This is why the study of mineralogical conditions of the ore, evaluating the effect of an oxidation pretreatment with hydroxyl ion (ammonia in solution -NH4OH), in gold recovery, will make possible the optimization of leaching with thiosulfate solutions (amoniaco en solución (S2O3), cobre-(II) (Cu), amoniaco (NH3) y EDTA.

Different authors have presented reaction mechanisms to explain the process of leaching and dissolving gold with thiosulfate (Breuer & Jeffrey, 2000, Senanayake, 2004) showing how the oxidation of gold, and therefore its dissolution, is catalyzed by the presence of the ion cupric (Cu2 +). Once the gold is oxidized by the presence of Cu2 + ions, the formation of the gold-thiosulfate complex is favored (Au(S2O3)2).

The objective of this work was to evaluate the mineralogy and the oxidation of the mineral in the process of leaching gold from refractory minerals with thiosulfate solutions through analytical techniques such as Polarized Flat Light Microscopy (MOLPP), Digital Image Processing (TDI), Scanning Electron Microscopy (SEM / EDS), X-ray Diffraction (XRD) and electrochemical techniques for the study of thiosulfate solution.

Materials and methods

Preparation of samples

The material used in this study was provided by the Provincial Center for Agro-entrepreneur Mining Management of northeast Antioquia; La Primavera mine, municipality of Segovia. This material was selected for its refractoriness and gold content, which was previously calculated using the fire test technique (representative tenors of the region 59 gAu / ton and 70 gAg / ton), and subjected to a comminution cycle until obtain a particle size (~ 75µm), passer Tyler 200 mesh.Toobtainthe samples, 180g of the study material were subjected to a thiosulfate leaching process and an oxidant pretreatment. In order to evaluate the effects of the leaching process, assemblies of epoxy resin grains were made, which were polished and polished until obtaining a surface with a mirror-like finish. This preparation was carried out with the leached samples and those not leached.

Leaching of refractory ore

The study material was subjected to different tests (A and B) of gold leaching with thiosulfate solutions, the effect of the oxidant pre-treatment, prior to leaching, was evaluated, where solutions of hydroxyl ion with bubbling were used (test B) and without air bubbling (test A). For the leaching of the gold material with thiosulfate, this was prepared with an oxidant pretreatment in ammonium hydroxide solution. In the oxidation pretreatment, a solution of 500 ml of ammonium hydroxide (0.8 mol / L) and copper sulfate (0.025 mol / L) was used. The solution and the mineral were poured into a closed glass cell and left for 12 hours with and without air bubbling. During leaching, ammonium thiosulfate (0.2 mol / L) and EDTA (0.025 mol / L) were added to the oxidizing solution, adjusting the pH to 10. The system was left in a closed glass cell with mechanical agitation for 24 hours at 250 rpm. Likewise, leaching tests were carried out without oxidation pre-treatment to compare the corrosion of the ore. All the leaching experiments were carried out at room temperature and the system was compared as a base point with the solution from a gold sheet of high purity (99.99% Au).

Caracterización mineralógica

The mineralogical characterization of the samples was carried out using the point counting technique, following the ASTM D 2799 standard, using a polarized flat light optical microscope, reflected light mode, Carl Zeiss AXIO SCOPE-A1-POL, with chromatic correction and compensation of flat image, with the objective of increasing air at 20X (ASTM, 2012). In addition, the point count was validated using TDI using the open source software ImageJ v.1,50b. The recognition of the mineral phases in a total of 3 polished sections allowed to identify up to a maximum of ~ 25,000 crystals per section (800 micrographs in total) with a confidence level of 95% and an error rate of 3%, thus guaranteeing the Reliability of the results with a greater statistical probability. The acquisition of images for the TDI was made leaving 2 mm of separation between images to avoid the overlap of the same; subsequently the images were converted to 8-bit format in gray scale and

normalized in order to improve the contrast. The separation and identification of each mineral phase was done using the threshold tool in ImageJ, assigning a range of values in the gray scale, eg, Au 254-255 bits, Py 180-253 bits, Cpy 178-179 bits, Gn 94 -177 bits, Sp 40-93 bits, Qz 20-39 bits. Finally, variables such as area, perimeter, Feret diameter, and circularity were used.

To determine the percentage of corrosion in each sample, characteristics such as grooves and pores observed in a total of 131 crystals were analyzed, among them, pyrite, sphalerite and galena. In the crystals, the Focus Stacking technique was used in order to improve the observation conditions, decreasing the effect of the depth of field (total of micrographs used, 790). The micrographs used for the corrosion analysis were obtained with the 100X lens of the AXIO SCOPE-A1-POL. The percentage of corrosion of each crystal was determined from the area and perimeter of both the crystal and the corroded zone (Figure 8).

We also used a DRX brand Panalytical Reference X'Pert PRO MPD with Cu radiation wavelength Kα = 1.5406, polarized with a power of 45 kV and 40 mA, continuous sweep with step of 0.013 ° and 59 seconds per step ; the database COD (Crystallography Open Database) was used for the identification of the crystalline phases in the samples. For the microchemical analysis, as well as the microtextural evolution, a SEM JEOL JSM 6490 LV was used, with an OSFORD type EDS solid state detector, in BSE observation mode and 20kV acceleration voltage and a collection time of 210 seconds. The samples were previously assembled in polished sections and metallized with gold.

Results and Discussion

Gold foil leaching

Figure 1 shows the result of leaching with the electrolyte from a gold foil (99.99% purity) in solutions of ammonium thiosulfate and sodium thiosulfate as baseline. In the ammonium thiosulfate solution after 15 hours of leaching, a solution of 24.8 mg of gold was reached; while in the sodium thiosulfate solution a solution of 8.0 mg was obtained; three times less than the ammonium thiosulfate solution. After 24 hours of leaching, a solution of 27.4 mg Au was obtained with the thiosulfate solution of ammonium and with the sodium thiosulfate solution alone 9.0 mg Au. According to the results obtained, with the solutions of sodium thiosulfate and ammonium thiosulfate the gold dissolved; however, the leaching kinetics of ammonium thiosulfate was higher, which results in shorter gold dissolution times for a leaching process using this thiosulfate salt.

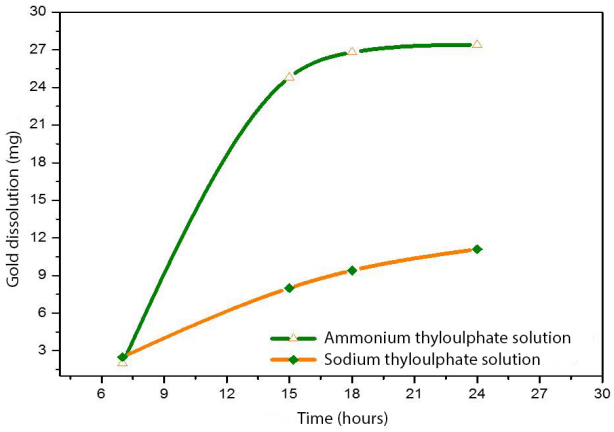

Figure 1. Gold foil solution (99.99% Au) in solutions of ammonium thiosulfate and sodium thiosulfate with ammonia, copper and EDTA at pH 10.2 with agitation for 24 hours at 500 rpm.

Electrodeposition Tests

With the gold concentration solution known and prepared from the gold foil, cyclic voltammetry tests were performed on platinum electrodes, to identify the potentials where gold reduction occurs (0.0014 M). In the voltammogram obtained (Figure 2A), the characteristic oxidation peaks of Cu0 / Cu1 + and Cu1 + / Cu2 + are observed and those of reduction of Cu2 + / Cu1 + and Cu1 + / Cu0; these responses (oxidation and reduction peaks) were previously defined and identified in electrochemical tests with the leaching electrolyte without gold solution (0.2 M (NH4) 2S2O3, 0.6 M NH3, 0.05 Cu (II) and 0.025M EDTA). Now, when there is dissolved gold in the leaching solution, in the voltammogram obtained (Figure 2B), three new peaks appear in the cathodic direction of the cyclic voltammetry, which are associated with the reduction of gold (Au). To verify this theory, we take the values of the new peaks observed at potentials E vs Ag / AgCl = -0.241 V, -0.343 V and -0.376 V and apply constant reduction potentials on a platinumelectrode.

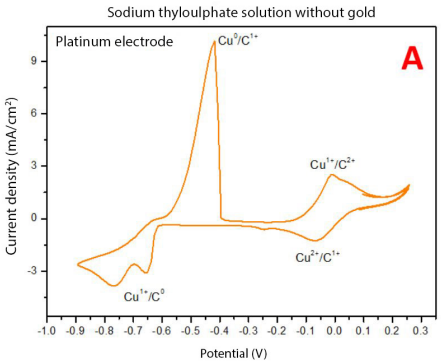

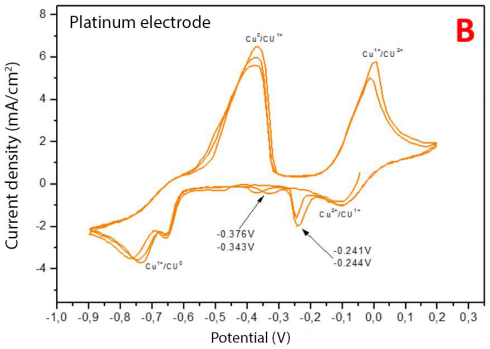

Figure 2. Cyclic voltammetry with potential scanning in negative direction at 10 mV / s on platinum electrode in solution of: A) 0.2 M (NH4) 2S2O3; 0.6 M NH3; 0.05 Cu (II); 0.025M EDTA and B) 0.2M (NH4) 2S2O3; 0.6 M NH3; 0.05 Cu (II); 0.025M EDTA + 0.0014 M Au. E vs Ag / AgCl.

Leaching tests of the auriferous mineral

Table 1 shows the leaching results. In tests A and B with gold content of 59.0g / ton and with a pretreatment of oxidation of the ore, gold solutions of 51.91% and 81.57% were obtained. In addition, test B (with air), presented greater dissolution of gold, during the pretreatment of oxidation of the mineral. These results show higher gold dissolution when an oxidation pretreatment (in ammonium hydroxide with air bubbling) of the ore is carried out before the leachate with thiosulfate, copper (II) solution, ammonia and EDTA.

Table 1. Gold dissolution of refractory minerals. Leaching for 24 hours with mechanical agitation (250 rpm). PTO: Pretreatment of oxidation in ammonium hydroxide; PTO + A: Pretreatment of oxidation in ammonium hydroxide + air.

Test	Condition	Tenor	Recovered (mg/L)	% of goldin solution
A	Con PTO	59.0 gAu/ton de mineral	18.48	51.91 %
B	Con PTO +A		29.04	81.57 %

Source: Authors

Initial mineralogical characterization

Through the techniques of manual point counting and TDI, for the sample M3 (without leaching process), the pyrite 58% (Py / FeS2), galena 15% (Gn / PbS), sphalerite 3% (Sp / ZnS), chalcopyrite 2% (Cpy / CuFeS2), arsenopyrite 2% (Aspy / FeAsS), free gold ~ 1% (Au) and quartz 19% (Qz / SiO2) (Figure 3, Table 2). Other mineral phases, by their size, shape, and quantity were defined by complementary techniques such as SEM / EDS and DRX. Additionally, euhedral and subhedral crystals of pyrite were observed, with square shapes characteristic of their isometric crystallization (Figures 3B and 4A). The surfaces observed are smooth, some fractured and with net contacts between crystals. In some areas there are fine-granular aggregates with anhedral crystallization (Figure 3A).

The largest crystals showed inclusions of sphalerite with subhedral to anhedral crystallization, mostly, although it also occurs in a lower proportion in the euhedral form. The gangue crystals appeared euhedral, possibly quartz in its basal cut. The sphalerite grains presented inclusions of chalcopyrite in the form of grains in specific areas of the sample and as inclusions, this type of sphalerite is known as sphalerite disease (Figure 4D). In addition, homogeneous and little massive crystals, without fractures, of arsenopyrite in fine droplets were observed, due to the size no marked anisotropy was observed, the cut was almost isometric (Figure 3D). Some grains of sphalerite presented inclusions of small crystals of galena. The gangue was presented in very few quantities. The galena presented euhedral and subhedral crystallization, good cleavage and characteristic triangular pits (Figure 4C). The galena was in contact with pyrite subhedral and anhedral, which was also present in inclusions, very fractured and crossed by very fine galena veins in cleavage planes. Galena grains were also found in contact with sphalerite and arsenopyrite in small droplets in the sphalerite matrix. The estimated percentage for this mineral is less than 5% of the total of the present phases.

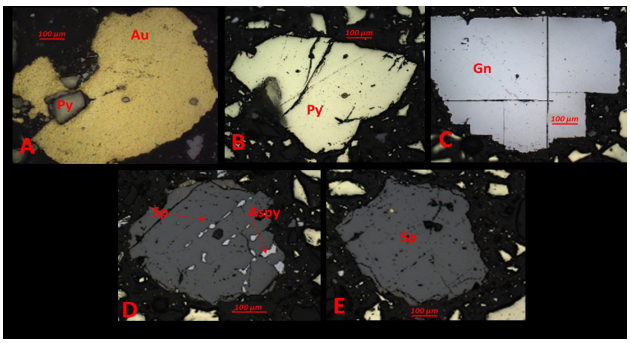

Figure 3. Sample M3 (without leaching process): (A) Free gold crystal, (B) Subhedral pyrite crystal, (C) Galena crystal with perfect 90 ° cleavage, (D) Arsenopyrite crystals as inclusions in sphalerite, and (E) Sphalerite crystal.

Tabla 2. Resultados de la caracterización por conteo de puntos manual y TDI.

	Muestra M3			Muestra A			Muestra B		
Fases Minerales	**Conteo de puntos Manual (%)**	Área (%)	**Diámetro de Feret** (µm)	**Conteo de puntos Manual (%)**	Área (%)	**Diámetro de Feret** (µm)	**Conteo de puntos Manual (%)**	Área (%)	**Diámetro de Feret** (µm)
FeS_2	58	51,9	61,88±31	0	36	35,44±19	55	12,8	37,8±12
PbS	15	26,5	77,27±54	0	0	0	9	15,7	44,05±16
ZnS	3	8,4	76,69±47	5	24	57,31±38	0	0	0
Au	1	1,3	49,38±17	0	0	0	0	26,8	47,51±23
AsFeS	2	0	0	0	0	0	0	0	0
CuFeS	2	0	0		0	0	0	0	0
SiO_2	19	11,9	57,86±32	30	40	62,49±36	0	44,7	55,49±32
TOTAL	**100**	**100**	-	**100**	**100**	-	**100**	**100**	-

Fuente: Autores

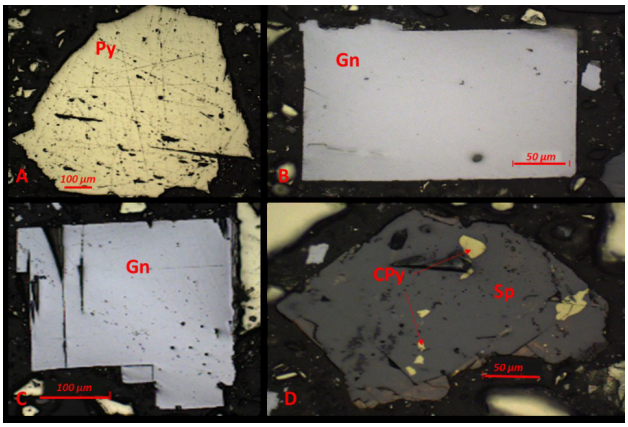

Figure 4. Sample M3 (without leaching process): (A) Subhedral pyrite crystal with square shape characteristic of its isometric crystallization, (B) Galena euhedral crystals with square shape, (C) Galena crystal with triangular pits of cleavage, and (D) Sphalerite crystal with inclusions of chalcopyrite.

Scanning electron microscopy (SEM-EDS)

The analysis of SEM in the samples showed the presence of intergrown quartz with grains of sphalerite disease (with inclusions of chalcopyrite) and pyrite mainly. The microchemical analyzes with EDS detector showed the presence of sphalerite with chalcopyrite in exsolution in the form of droplets. In general, sphalerite grains present substitution of Zn by Fe, but in a proportion not greater than 6% by weight(Figure5).

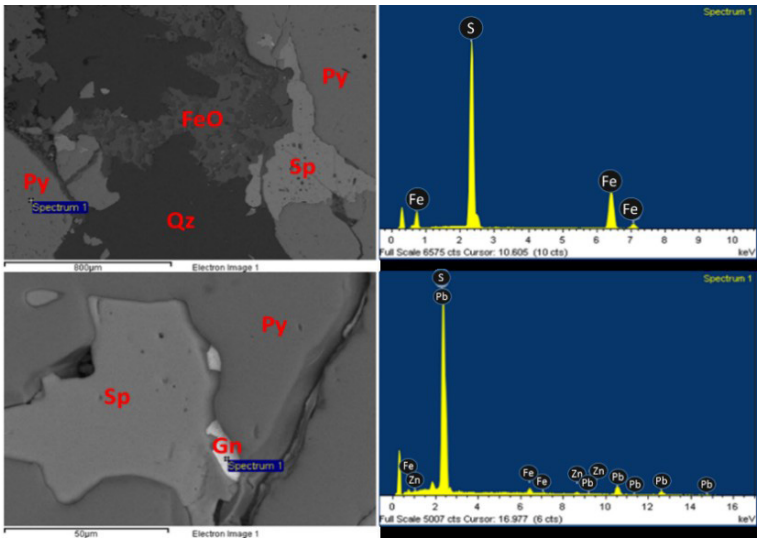

Figure 5. (above), pyrite crystals (Py, S = 42.89% and Fe = 57.11%), quartz (Qz, Si = 48.27% and O = 49.27%), sphalerite (Sp, Fe = 4) , 47%, Zn = 64.96% and S = 36.77%) and iron oxides (FeO, Fe = 53.52% and O = 50.70%), (lower), galena (Gn, Pb = 78.25% and S = 16.18%) intergrown with sphalerite crystals (Sp, Zn = 56.44%, Fe = 4.96% and S = 38.50%).

In addition, intergrowth of aluminum, manganese and magnesium feldspars was observed. The presence of minerals was evidenced that it was not possible to observe by other characterization techniques such as iron oxides (Figure 5) with some manganese inclusions. The proportions by weight according to the microchemical analyzes are O: 35.70%, Mn: 0.54 and Fe: 63.75%. Galena grains intergrown with sphalerite grains were found, as well as well-defined crystals of arsenopyrite included within the sphalerite (Figure 5).

X-ray diffraction (XRD)

The technique allowed to identify the crystalline phases accompanying the pyrite, as well as their relative abundances. Pyrite, galena, sphalerite, quartz, and traces of a cadmium sulfide identified as Greenockite were identified (Figure 6).

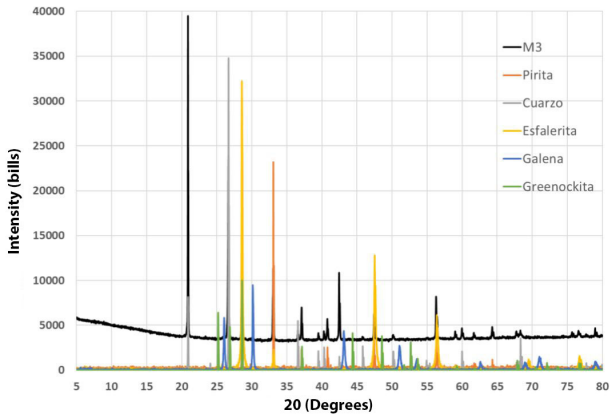

Figure 6. XRD where reflections of pyrite, quartz, galena and sphalerite were identified.

TDI granulometric analysis

To determine the particle size, a granulometric distribution study was carried out using TDI (Figure 7). As the mechanical analysis depends on the measurement of the mass of the particles, the TDI depends on the measurement of morphological parameters (area, length, width and equivalent diameter) and the number of particles. The study was performed using the Feret diameter of each particle thrown by the ImageJ software, although this is somewhat difficult to determine experimentally with precision. The diameter of Feret is determined by the random orientations that the particles can take. In addition, both Feret diameter and mechanical analysis are affected by the variety in the type of particle shapes (elongated, flat, spherical). However, by means of this analysis and form factors such as circularity, the behavior of the particles during the oxidation and electrolysis processes can be seen, particularly the connection between particle shape and property correlation.

It was possible to determine the most representative particle size and its behavior related to the oxidation and dissolution processes. The results obtained are supported by statistics determining the average diameter in a population of between 400 and 5000 particles.

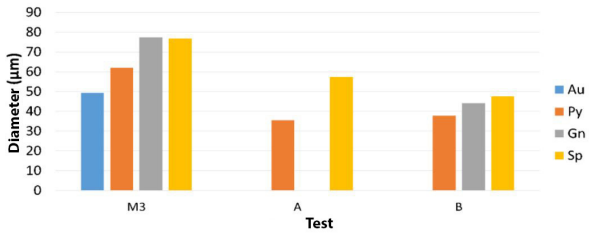

Figure 7. Behavior of feret diameter for each mineral phase in the samples analyzed.

Trial A

In Figures 8D-F, pyrite crystals were observed with poor evidence of corrosion, although with a visible reduction in size, accumulations of pyrite grains were estimated in nodules of varying sizes between approximately 300 and 500 µm, as well as separate grains. individually of approximate size of 40-80 µm. With the TDI it was determined that this sample presented very little corrosion, between 1% and 4% of corroded area. The pyrite grains showed a pale yellow color without anisotropy and unequal, and by the dissolution processes are observed anhedra and sub-rounded. As in the previous tests, the almost total dissolution of accompanying mineral phases such as arsenopyrite, chalcopyrite and galena was shown, which represent about 5% of the sample and the presence of some aluminosilicates that represent 30% of the sample. Also, the presence of iron and copper precipitates was observed as a product of the leaching process.

Trial B

Trial B showed the highest percentage of gold dissolution, 81.57%. Pyrite grains of pale yellow color were observed with unequal crystals ~ 40-75 µm. The amount and size of generalized pores and large grooves in some crystals increased greatly, representing up to 36% of corroded area (Figure 8A-C). Pyrite represents 55% of the sample.

Additionally, light gray galena crystals are also anhedral with evidence of corrosion and dissolution, this time not limited to the planes of mineral weakness and large pores. In addition, galena was found coating pyrite crystals and in some cases with inclusions of chalcopyrite and arsenopyrite. The sphalerite occurs in a lesser proportion in dark gray grains with anhedral and unequal crystals showing evidence of corrosion as in the previous crystals and with inclusions of chalcopyrite crystals. The presence of crystals of aluminosilicates is also noticeable in a large proportion, although of smaller size compared to the previous tests, showing crystals of siderite (iron carbonate) which according to Feng and van Deventer (2007) favors the process of gold recovery , increasing the concentration of this mineral by 10%. This carbonate represents 20% of the sample.

On the other hand, by means of XRD (Figure 9) the relative decrease of the accompanying phases of pyrite was evidenced, even diminishing the relative intensity of the pyrite. Part of the present galena was given by dissolution of the pyrite which allowed the ore to come out. In addition, the SEM analysis (Figure 10) revealed the presence of intergrown quartz with grains of sphalerite disease and pyrite mainly, these trials are in accordance with the MOLPP analyzes. In order to define the chemical composition of the grains, a microchemical analysis was performed with an EDS detector to each of the grains, finding pyrite, intergrown with quartz grains, and galena grains intergrown with grains of sphalerite that presents traces in turn of Cd.

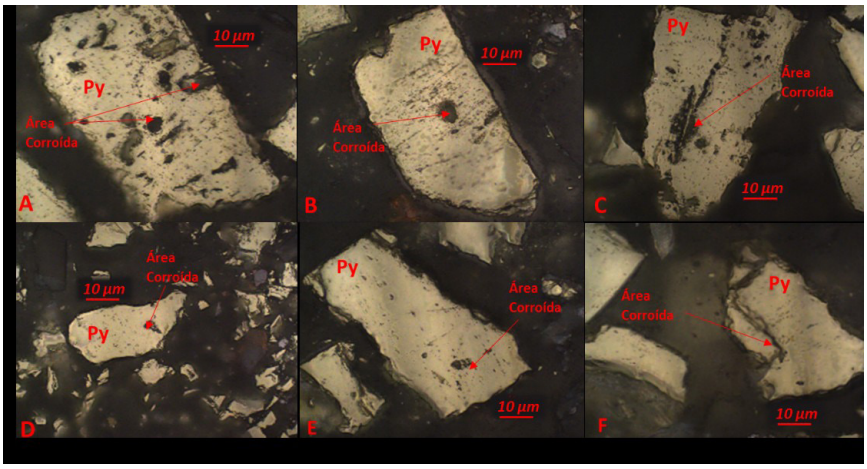

Figure 8. General overview at 100X: Test A (D, E and F), Test B (A, B and C).

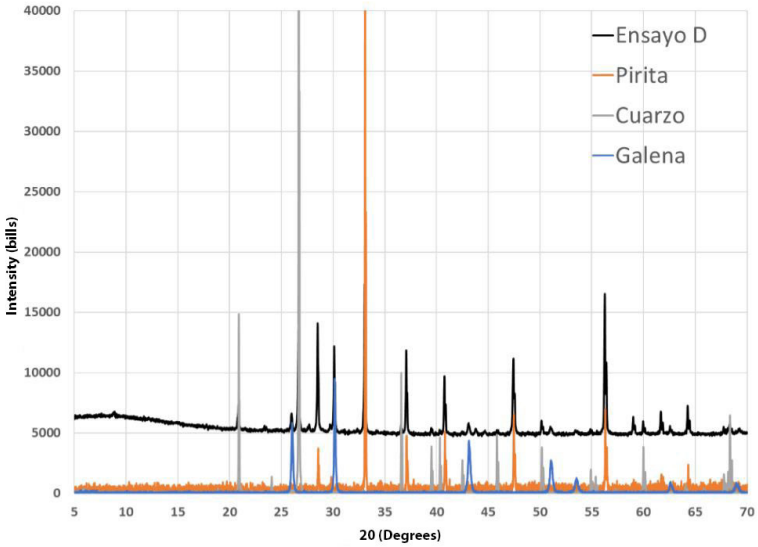

Figure 9. XRD where the reflections of the crystalline phases were identified after the oxidation and leaching process, predominating pyrite, galena and quartz.

The results obtained are in agreement with that found by Feng and Van Deventer (2002) where it was reported that dissolution in media with thiosulfate is given in the following order: chalcopyrite> galena> pyrrhotine> sphalerite> arsenopyrite> pyrite. This may be due to the formation of galvanic pairs of sulphides in contact, favoring the dissolution of sulfur with less potential of rest. For example, it has been reported that the sphalerite in contact with chalcopyrite favors the dissolution of the sphalerite and that the sphalerite in contact with galena favors the dissolution of the latter (Mejía, Ospina, Márquez, & Morales, 2009; Urbano, Meléndez, Reyes , Veloz, González, 2007).

On the other hand, being the pyrite the predominant mineral in the samples, the reduction in the dissolution of gold in the ammoniacal solutions was possibly the one that catalyzed the decomposition of thiosulfate in tetrathionate as found by Feng and van Deventer (2006) in conjunction with the addition of sulphate in a system with pyrite increases the Dissolution speed of gold. Despite the decrease, gold recoveries of over 80% were achieved. In this test the dissolution of the accompanying sulfides favors the generation of sulphate in the medium, which allows the pyrite to be depressed and the gold solution in the leachingsystem.

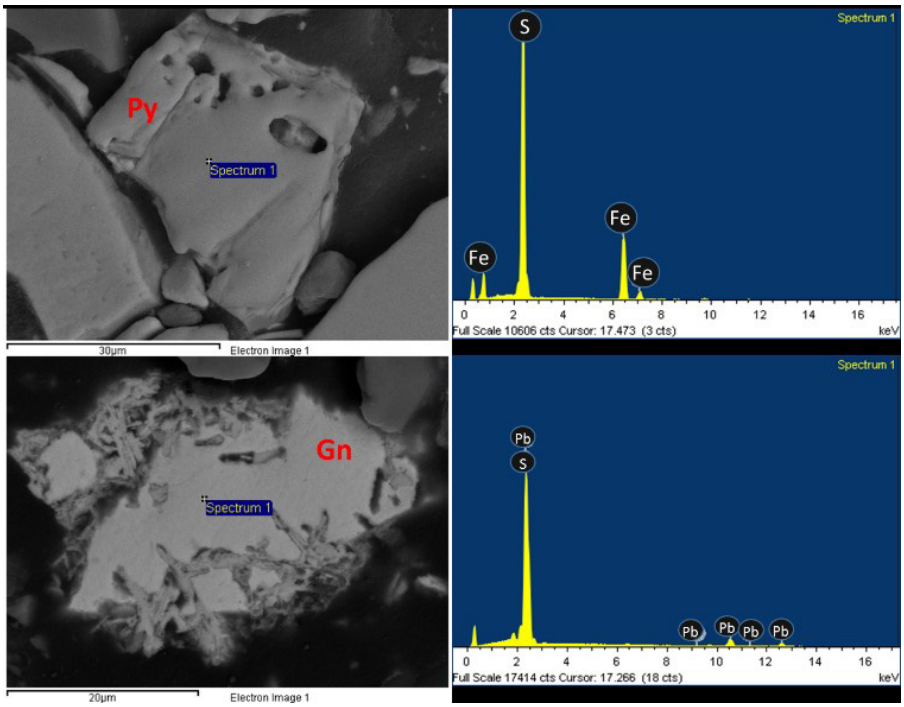

Figure 10. Image of SEM and EDX showing: (top), a grain of pyrite (Fe = 44.27% and S = 55.73%) (Spectrum 1) with evidence of pores and corrosion grooves; (lower), a grain of galena (Pb = 86.66% and S = 13.34%) (Spectrum 1) with evidence of predominant corrosion in the planes of mineral weakness (Clivaje).

The formation of iron hydroxides has been reported by Feng and van Deventer (2006, 2007a) as the cause of the passivation of the dissolution process with thiosulfate due to the formation of a superficial layer on the sulfides and gold grains that impede the process of dissolution, in addition to generating the thiosulfate decomposition. This effect is more marked in large concentrations of hematite. In agreement with this, in the trials where the highest iron oxide formation was observed, the gold solution was lower. Additionally, the chalcopyrite solution of the mineral concentrates increases the content of the Cu2 + ion in solution, so its concentration must be controlled in the dissolution processes with thiosulfate. This ion, although it has been reported by Breuer and Jeffrey (2000) and Senanayake (2004) as a catalyst of the process, in large concentrations it can precipitate as copper sulphides and inhibit the gold release process, due to its formation in layers over the surface of free gold or of the mineral to dissolve (Feng & van Deventer, 2007c).

It has also been reported that sulfide concentrates with presence of carbonates and manganese dioxides favor the process of leaching gold with thiosulfate, however, a high amount of these generates overconsumption of thiosulfate which could make the process more expensive and unfeasible (Feng & van Deventer, 2007b). The

mineralogical characterization of the sulphide concentrates used showed a low concentration of these minerals, which could favor the dissolution of gold.

On the other hand, the XRD of the samples before and after the process showed a decrease in the characteristic peaks of the sulfides present in the concentrate associated with the decrease of these phases, which was corroborated by optical microscopy and SEM where after the process of leaching with thiosulfate was observed the decrease of chalcopyrite, arsenopyrite, sphalerite, galena and evidence of corrosion in pyrite grains. This superficial alteration in the form of pores, grooves and corrosion pits after the pre-treatment process Leaching with thiosulfate facilitates access of the thiosulfate solution to the mineral and thus to the gold particles (Feng & van Deventer, 2010). On the other hand, preferential corrosion in fracture zones due to grinding or cleavage is observed in all tests. This is in accordance with that reported by (Bennett & Tributsch, 1978, Urbano, Meléndez, Reyes, Veloz, González 2007), since these areas have a more favorable potential or are more chemically reactive because they have a higher surface energy and They oxidize easily.

Finally, some minerals, such as aluminosilicates, present in the concentrate remained unchanged, demonstrating the refractoriness or inertia of these in this type of process. These results are in agreement with those reported by (Mejía, Ospina, Márquez & Morales 2007).

Conclusiones

The mineralogical characterization allowed to define the ranges of potentials suitable for the recovery of gold, since the dissolution of the various accompanying phases varies with the currents required for the electrolixiviation of gold. So then, the dissolution process with thiosulfate, in addition to the potential, depends on the mineralogical proportion of the initial simple.

Both solutions, sodium thiosulfate and ammonium thiosulfate, dissolve the gold; however, the leaching kinetics of ammonium thiosulfate was higher, which results in shorter gold dissolution times for a leaching process using this thiosulfate salt.

When there is dissolved gold in the leaching solution, in the voltammogram three new peaks appear in the cathodic direction of the cyclic voltammetry, which are associated with the reduction of gold (Au).

In Trials A and B with gold content of 59.0g / ton and with a pretreatment of oxidation of the ore, gold solutions of 51.91% and 81.57% were obtained. In addition, test B (with air), presented greater dissolution of gold, during the pretreatment of oxidation of the mineral. These results show greater gold dissolution when an oxidation pretreatment (in ammonium hydroxide with air bubbling) of the ore is carried out before the leachate with thiosulfate, copper (II), ammonia and EDTA solution.

The amount and size of the generalized pores, and large grooves in some crystals increase in a large proportion, representing up to 36% of área corroded, as a consequence of the oxidation treatment of the mineral.

The XRD technique showed the relative decrease of the phases accompanying the pyrite, even decreasing the relative intensity of the pyrite, and part of the galena present was given by dissolving the pyrite which allowed the ore to exit. This was corroborated by optical microscopy and SEM where, after the process of leaching with ammonium thiosulfate, the decrease in chalcopyrite, arsenopyrite, sphalerite, galena and evidence of corrosion in pyrite grains was observed.

The formation of galvanic pairs between sulphides in contact, favors the dissolution of sulfur with lower resting potential, showing results according to the literature where it is reported that dissolution in media with thiosulfate is given in the following order chalcopyrite> galena> pyrrhotine> sphalerite > arsenopyrite> pyrite.

The mineralogical characterization of the sulphide concentrates used showed a low concentration of these minerals, which could favor the dissolution of gold.

Surface alteration in the form of pores, grooves and corrosion pits after the pre-treatment process prior to thiosulfate leaching, facilitates access of the thiosulfate solution to the mineral and thus to the gold particles. On the other hand, in all the tests preferential corrosion is observed in fracture zones due to grinding or cleavage; since these zones have a more favorable potential or are more chemically reactive because they have a higher surface energy and are easily oxidized.

When there is dissolved gold in the leaching solution, in the voltammogram three new peaks appear in the cathodic direction of the cyclic voltammetry, which are associated with the reduction of gold (Au)....

Copper is one of the most important catalysts in these processes, therefore it is necessary to track the various copper minerals within the sample, before and after the process, since large amounts of copper in solution could lead to its precipitation as an amorphous phase and inhibit gold leaching.

The mineralogical characterization by TDI allowed to identify and quantify different mineral phases present in the samples in a much more efficient and economic way. The results are favored by statistics by using a much larger number of micrographs and crystals. The variation presented by the different samples to be subjected to the electrolysis process. An average of 49% phase dissolution was determined, such as galena, pyrite and chalcopyrite. Pyrite presented an average of 8% corrosión.

With previous results obtained in the leaching tests of a gold foil, the leaching power of the ammoniacal thiosulfate solution to dissolve and complex gold is demonstrated. The pretreatment of oxidation of the mineral with ammonium hydroxide solution, showed a good result evidencing points and grooves of corrosion in the different grains observed through its reconstruction with the focus stacking technique. In addition, with this oxidation treatment the gold solution in the leaching solution is increased.

The best conditions for the leaching of the ore, with a gold release of 51.91% and 81.57%, were achieved with a pretreatment of the mineral in ammonium hydroxide solution and copper for 12 hours with air bubbling, followed by leaching in solution of ammonium thiosulfate and EDTA at pH between 10.2 and 10.3, for a period of 24 hours with mechanical agitation at 250 rpm.

In the electrodeposition tests from a known gold solution of ammonium thiosulfate, copper, ammonia, EDTA and gold, potentials were found where the reduction or recovery of dissolved gold occurs (E vs Ag / AgCl = -343 mV and -376 mV). Although in these potentials a co-deposit of silver and copper is also observed.

Acknowledgments

To the laboratories of the University of Antioquia CIDEMAT and Mineralurgia, to the Operational Direction of Investigation, DOI, of the Pascual Bravo University Institution for the partial financing of this work, to the members of the seedbed of research SIA and of the Research and Innovation Group Environmental GIIAM, and especially to *Empresas Públicas de Medellín* for the financial support.

References

Abrantes, L. M., & Costa, M. C. (1996). Electro-oxidation as a pretreatment for gold recovery. *Hydrometallurgy*, *40*(1-2), 99–110. http://doi.org/10.1016/0304-386X(94)00077-G

Adams, M. D. (2005). Advances in Gold Ore Processing. *Developments in Mineral Processing*, *15*, 994–1013. http://doi.org/10.1016/S0167-4528(05)15041-8

Amankwah, R. K., & Pickles, C. A. (2009). Microwave roasting of a carbonaceous sulphidic gold concentrate. *Minerals Engineering*, *22*(13), 1095–1101. http://doi.org/10.1016/j.mineng.2009.02.012

ASTM. (2012). Standard Test Method for Microscopical Determination of the Maceral Composition of. *ASTM International*, *D2799–11*, 1–6.

Awe, S. A., & Sandstrom, K. (2010). Selective leaching of arsenic and antimony from a tetrahedrite rich complex sulphide concentrate using alkaline sulphide solution. *Minerals Engineering*, *23*(15), 1227–1236. http://doi.org/10.1016/j.mineng.2010.08.018

Baláž, P, Achimovičová, M. (2006). Selective leaching of antimony and arsenic from mechanically activated tetrahedrite, jamesonite and enargite. *International Journal of Mineral Processing*, *81*(1), 44–50. http://doi.org/10.1016/j.minpro.2006.06.004

Bennett, J. C., & Tributsch, H. (1978). Bacterial leaching patterns on pyrite crystal surfaces. *Journal of Bacteriology*, *134*(1), 310–317.

Breuer, P. L., & Jeffrey, M. I. (2000). Thiosulfate leaching kinetics of gold in the presence of copper and ammonia. *Minerals Engineering*, *13*(10), 1071–1081. http://doi.org/10.1016/S0892-6875(00)00091-1

Celep, O., Alp, I., & Deveci, H. (2011). Improved gold and silver extraction from a refractory antimony ore by pretreatment with alkaline sulphide leach. *Hydrometallurgy*, *105*(3-4), 234–239. http://doi.org/10.1016/j.hydromet.2010.10.005

Celep, O., Alp, I., Paktune, D., & Thibault, Y. (2011). Implementation of sodium hydroxide pretreatment for refractory antimonial gold and silver ores. *Hydrometallurgy*, *108*(1-2), 109–114. http://doi.org/10.1016/j.hydromet.2011.03.005

Chen, T., Cabri, L., & Dutrizac, J. (2002). Characterizing gold in refractory sulfide gold ores and residues. *Jom*, *54(12)*(December), 1–3. Retrieved from http://link.springer.com/article/10.1007/BF02709181

Climo, M., Watling, H. R., & Van Bronswijk, W. (2000). Biooxidation as pretreatment for a telluride-rich refractory gold concentrate. *Minerals Engineering*, *13*(12), 1219–1229. http://doi.org/10.1016/S0892-6875(00)00106-0

Córdoba, E. M., Muñoz, J. A., Blázquez, M. L., González, F., & Ballester, A. (2008). Leaching of chalcopyrite with ferric ion. Part I: General aspects. *Hydrometallurgy*, *93*(3-4), 81–87. http://doi.org/10.1016/j.hydromet.2008.04.015

Corkhill, C. L., & Vaughan, D. J. (2009). Arsenopyrite oxidation - A review. *Applied Geochemistry*, *24*(12), 2342–2361. http://doi.org/10.1016/j.apgeochem.2009.09.008

Feng, D., & Van Deventer, J. S. J. (2002). Leaching behaviour of sulphides in ammoniacal thiosulphate systems. *Hydrometallurgy*, *63*(2), 189–200. http://doi.org/10.1016/S0304-386X(01)00225-0

Feng, D., & van Deventer, J. S. J. (2006). Ammoniacal thiosulphate leaching of gold in the presence of pyrite. *Hydrometallurgy*, *82*(3-4), 126–132. http://doi.org/10.1016/j.hydromet.2006.03.006

Feng, D., & van Deventer, J. S. J. (2007a). Effect of hematite on thiosulphate leaching of gold. *International Journal of Mineral Processing*, *82*(3), 138–147. http://doi.org/10.1016/j.minpro.2006.09.003

Feng, D., & van Deventer, J. S. J. (2007b). Interactions between sulphides and manganese dioxide in thiosulphate leaching of gold ores. *Minerals Engineering*, *20*(6), 533–540. http://doi.org/10.1016/j.mineng.2006.10.012

Feng, D., & van Deventer, J. S. J. (2007c). The effect of sulphur species on thiosulphate leaching of gold. *Miner. Eng*, *20, no. 3*, 273–281.

Feng, D., & van Deventer, J. S. J. (2010). Oxidative pretreatment in thiosulphate leaching of sulphide gold ores. *International Journal of Mineral Processing*, *94*(1-2), 28–34. http://doi.org/10.1016/j.minpro.2009.11.002

Gudyanga, F. P., Mahlangu, T., Roman, R. J., Mungoshi, J., & Mbeve, K. (1999). Acidic pressure oxidation pretreatment of refractory gold concentrates from the Kwekwe roasting plant, Zimbabwe. *Minerals Engineering*, *12*(8), 863–875. http://doi.org/10.1016/S0892-6875(99)00074-6

Hashemzadehfini, M., Ficeriová, J., Abkhoshk, E., & Shahraki, B. K. (2011). Effect of mechanical activation on thiosulfate leaching of gold from complex sulfide concentrate. *Transactions of Nonferrous Metals Society of China (English Edition)*, *21*(12), 2744–2751. http://doi.org/10.1016/S1003-6326(11)61118-7

Iglesias, N., & Carranza, F. (1996). Treatment of a gold bearing arsenopyrite concentrate by ferric sulphate leaching. *Minerals Engineering*, *9*(3), 317–330. http://doi.org/10.1016/0892-6875(96)00016-7

Klauber, C. (2008). A critical review of the surface chemistry of acidic ferric sulphate dissolution of chalcopyrite with regards to hindered dissolution. *International Journal of Mineral Processing*, *86*(1-4), 1–17. http://doi.org/10.1016/j.minpro.2007.09.003

Leng, F., Li, K., Zhang, X., Li, Y., Zhu, Y., Lu, J.,& Li, H. (2009). Comparative study of inorganic arsenic resistance of several strains of Acidithiobacillus thiooxidans and Acidithiobacillus ferrooxidans.

Hydrometallurgy, *98*(3-4), 235–240. http://doi.org/10.1016/j.hydromet.2009.05.004

Márquez G., M. A. (1999). *Mineralogia dos processos de oxidacao sobre pressao e bacteriana do minerio de ouro da mina Sao Bento, MG*. Tese de doutorado. Universidad de Brasilia.

Márquez, M. (1995). *Caracterização mineralógica do minério, concentrado e rejeito da flotação da mina São Bento.* Universidade de Brasília. Instituto de Geociências.

Marsden, J. O., & House, C. I. (2009). The chemistry of gold extraction. 2d ed. *Metallurgy and Exploration*, 42–44,111–126,161–177,191–193,233–263,297–333.

Mejía, E. R., Ospina, J. D., Márquez, M. A., & Morales, L. (2007). Bioleaching of Galena (PbS). *Fourier Transform - Materials Analysis*, 191– 206.

Mejía, E. R., Ospina, J. D., Márquez, M. A., & Morales, A. L. (2009). Oxidation of chalcopyrite (CuFeS 2) by Acidithiobacillus ferrooxidans and a mixed culture of Acidithiobacillus ferrooxidans and Acidithiobacillus thiooxidans like bacterium in shake flasks. *Materials Research*, *73*, 385–388. http://doi.org/10.4028/www.scientific.net/AMR.71-73.385

Mesa Espitia, S. L., & Lapidus, G. T. (2015). Pretreatment of a refractory arsenopyritic gold ore using hydroxyl ion. *Hydrometallurgy*, *153*, 106–113. http://doi.org/10.1016/j.hydromet.2015.02.013

Muir, D., & Aylmore, M. (2005). Thiosulfate as an alternative lixiviant to cyanide for gold ores. *Dev. Miner. Process*, *vol. 15*, 541–60.

Rohwerder, T., & Sand, W. (2003). The sulfane sulfur of persulfides is the actual substrate of the sulfur-oxidizing enzymes from Acidithiobacillus and Acidiphilium spp. *Microbiology*, *149*(7), 1699–1709. http://doi.org/10.1099/mic.0.26212-0

Senanayake, G. (2004). Analysis of reaction kinetics, speciation and mechanism of gold leaching and thiosulfate oxidation by ammoniacal copper(II) solutions. *Hydrometallurgy*, *75*(1-4), 55–75. http://doi.org/10.1016/j.hydromet.2004.06.004

Tongamp, W., Takasaki, Y., & Shibayama, A. (2009). Arsenic removal from copper ores and concentrates through alkaline leaching in NaHS media. *Hydrometallurgy*, *98*(3-4), 213–218. http://doi.org/10.1016/j.hydromet.2009.04.020

Urbano, G., Meléndez, A.M., Reyes, V.E., Veloz, M.A., & Gonzáles, I. (2007). Galvanic interactions between galena – sphalerite and their reactivity. *International Journal of Mineral Processing*, *82*, 148–155. http://doi.org/10.1016/j.minpro.2006.09.004

Zhang Senanayake, G. & Nicol, M.J., X. M. (2004). The kinetics of the dissolution of gold colloid in oxygenated ammoniacal thiosulphate solutions. *Hydrometallurgy*, *74*, 243–257.

Zhang, X.-M. (2008). The dissolution of gold colloids in aqueous thiosulfate solutions. *Murdoch University*, (August). Retrieved from http://oatd.org/oatd/record?record={%}22oai:researchrepository.murdoch.edu.au:672{%}22